GLOBAL BIOGEOCHEMICAL CYCLES, VOL. 18, GB4017, doi:10.1029/2004GB002236, 2004

Disturbance and net ecosystem production across three climatically distinct forest landscapes

John L. Campbell, O. J. Sun, and B. E. Law
Department of Forest Science, Oregon State University, Corvallis, Oregon, USA

Received 10 February 2004; revised 10 August 2004; accepted 31 August 2004; published 5 November 2004.

[1] Biometric techniques were used to measure net ecosystem production (NEP) across three climatically distinct forest chronosequences in Oregon. NEP was highly negative immediately following stand-replacing disturbance in all forests and recovered to positive values by 10, 20, and 30 years of age for the mild and mesic Coast Range, mesic West Cascades, and semi-arid East Cascades, respectively. The response of stand-level NEP to individual disturbance events is greater than that attributable to edaphoclimatic differences between forest type. However, regional age class distributions are such that the variability in landscape-level NEP attributable to disturbance regimes is equivalent to that attributable to regional edaphoclimatic differences between forest types. Simulations of age class distribution under varying disturbance frequencies suggest that the sensitivity of landscape-level NEP to changes in disturbance regime varies among forest types and is linked to both remnant detritus and photosynthetic recovery rate that are partly a function of edaphoclimatic differences. *INDEX TERMS:* 1615 Global Change: Biogeochemical processes (4805); *KEYWORDS:* disturbance, forest carbon dynamics, net ecosystem production

Citation: Campbell, J. L., O. J. Sun, and B. E. Law (2004), Disturbance and net ecosystem production across three climatically distinct forest landscapes, *Global Biogeochem. Cycles*, *18*, GB4017, doi:10.1029/2004GB002236.

1. Introduction

[2] Net ecosystem production (NEP) can be defined as the difference between gross primary production and ecosystem respiration. Forests exhibiting negative NEP are acting as sources of atmospheric carbon, while forests exhibiting positive NEP are acting as sinks. Current concern over atmospheric CO_2 levels and subsequent global warming has brought the issue of forest NEP to the forefront of Earth science and challenged forest ecologists to quantify the impact of climate and disturbance on NEP, not only of individual forest stands but across entire forest landscapes. Climate is known to affect forest NEP by directly controlling the physiology of production and decomposition of organic matter [*Woodwell and Whittaker*, 1968; *Jarvis*, 1995].

[3] Conventional theory regarding the successional trends in NEP following disturbance is based on assumptions about the relative proportions of growing and decomposing tissue [*Odum*, 1969; *Sprugel*, 1985; *Harmon et al.*, 1990]. According to this theory (Figure 1, top), forests experience a pulse of negative NEP following catastrophic disturbances such as crown fire or clear-cutting, as these events both drastically reduce the amount of photosynthetic tissue and increase pools of respiring detritus. As living vegetation recovers and detrital pools decay, NEP becomes more positive, reaching a peak when detrital pools are near their lowest and production is near its highest. A subsequent decline in NEP occurs as interdisturbance mortality restocks detrital pools, which may or may not be compounded by declines in gross primary production.

[4] Recent studies suggest that the changes in stand-level NEP that occur as a result of disturbance, even without accounting for losses incurred during the disturbance event, may well exceed that attributable to either interannual variation in climate [*Thornton et al.*, 2002] or among-biome variation in climate [*Chapin et al.*, 2002]. However, when considering landscapes comprising stands in varying stages of regrowth, it is not immediately apparent how much variability in overall NEP is being caused by disturbance or how sensitive landscape NEP is to changes in the frequency of disturbance.

[5] As implied in Figure 1, the NEP of any forested landscape is constrained both by the successional trends in NEP and the age class distribution created by the prevailing disturbance regime [*Kurz and Apps*, 1999], and perhaps more important than the overall weighting of NEP by age class frequency is just how the amplitude and recovery rate of NEP renders a landscape more or less sensitive to alterations in age class distribution brought on by changes in disturbance regimes. After all, depending on the exact shape of the NEP curve in Figure 1, we would expect there to be age ranges where shifts in relative abundance would have little effect on landscape NEP as well as age ranges where shifts in relative abundance would profoundly alter landscape NEP.

0886-6236/04/2004GB002236$12.00

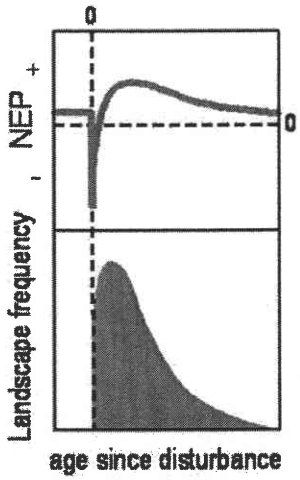

Figure 1. Theorized successional patterns in forest NEP following a stand-replacing disturbance. Disturbance regimes affect landscape-level NEP by defining the relative frequency of forest age classes.

[6] The robust chronosequence studies which aid in quantifying the influence of age class distribution on regional NEP are only now appearing in the literature. *Wirth et al.* [2002], *Bond-Lamberty et al.* [2004], *Howard et al.* [2004], and *Litvak and Miller* [2003] have all quantified age-related trends in NEP for boreal forests, while *Smith and Resh* [1999], *Janisch and Harmon* [2002], and *Law et al.* [2003] have reported age-related trends in temperate systems. Together, these studies help refine theories regarding successional trends in forest carbon exchange and provide valuable information regarding the response of stand-level NEP to disturbance. In this study we present values for NEP measured across multiple, replicated, edaphoclimatically distinct forest chronosequences and assess for each the capacity of disturbance to influence landscape-level NEP through current and alternative age class distributions. Specifically, our goals were to (1) quantify the successional trends in NEP that follow stand-replacing disturbance in each of three edaphoclimatically distinct conifer forests types in Oregon, (2) determine which component carbon fluxes were most responsible for the magnitude of NEP and which were most responsible for the trends in NEP, (3) compare the relative importance of disturbance and edaphoclimatic controls on regulating NEP at both individual stands and across entire landscapes, and (4) assess the sensitivity of landscape level NEP to alterations in disturbance regimes and link this sensitivity to the production biology of each forest type.

2. Methods

2.1. Study Design

[7] To assess successional trends in NEP across western Oregon, we selected 36 independent forest plots arranged as three replicates of four age classes in each of three edaphoclimatically distinct forest types. Each study plot encompassed 1 ha of structurally homogenous forest determined to be representative of its age and compositional type. The three forest types are located along a wide precipitation and elevation gradient and are best described as hemlock-Sitka spruce in the fog belt of Coast Range near Cascade Head Experimental Forest, Douglas fir in the West Cascade Mountains near H. J. Andrews Experimental Forest, and ponderosa pine in the Metolius basin in the dry east side of the Cascade Mountains. The locations of the study sites are shown in Figure 2, and the climatic, edaphic, and compositional characteristics of each site are given in Table 1. Forest ages range from 10 to 450 years and are subjectively classified as either initiation, young, mature, or old. Structural qualities of these age classes are described in Table 2.

2.2. Estimating NEP

[8] The mass balance approach for estimating NEP from field measurements begins in this study by separating the flow of gross photosynthate into three carbon allocation paths represented by equations (1) through (3).

$$NEP_{foliage} = NPP_{foliage} - litterfall, \quad (1)$$

where $NPP_{foliage}$ is the net primary production of tree, shrub, and herb foliage and litterfall is assumed to approximate the heterotrophic decomposition of dead leaves.

$$NEP_{wood} = NPP_{wood} - RH_{woody\ debris}, \quad (2)$$

where NPP_{wood} is the net primary production of the bole branches and bark of trees and shrubs, and $RH_{woody\ debris}$ is the heterotrophic respiration from fine and coarse woody debris.

$$NEP_{root} = \Delta \text{ coarse root} + \Delta \text{ fine root}, \quad (3)$$

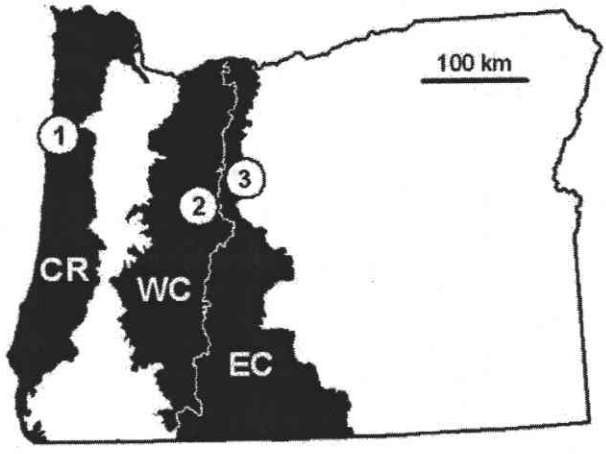

Figure 2. Geographic location of the study sites and the extent of the forest types they represent in western Oregon. Study sites are shown as 1–3. CR, Coast Range; WC, West Cascades; EC, East Cascades.

Table 1. Climatic, Edaphic, and Biological Characteristics of the Three Study Sites

Site Characteristic	Coast Range	West Cascades	East Cascades
Canopy composition (importance by basal area)	western hemlock (0.36)	Douglas fir (0.79)	ponderosa pine (0.95)
	Sitka spruce (0.34)	western red cedar (0.10)	
	Douglas fir (0.27)	western hemlock (0.10)	
Additional indicator species	red alder, vine maple, salmonberry, salal, red huckleberry, sword fern	vine maple, salal, red huckleberry, sword fern, Rhododendron	white fir, incense cedar, antelope bitterbrush, green leaf manzanita, Idaho fescue
Geographic location	Salmon River drainage of Tillamook county Oregon	Blue River drainage of Linn county Oregon	upper Metolius River of Deschutes county Oregon
Map coordinates	45.1°N 123.9°W	44.2°N 122.2°W	44.4°N 121.7°W
Elevation, m	120–300	710–860	890–1230
Precipitation (long-term average mm yr^{-1})	2800	2100	500
Mean Summer air temperature (long-term average C°)	14.5	14.1	14.5
Number of frost-free days	333	255	190
Soil description	basaltic colluvium forming well drained silt loams	igneous colluvium and residuum forming well drained stony clay loams	ash over colluvium forming well drained sandy to gravelly loams

where Δ coarse root and Δ fine root are the changes in each of these carbon pools over time, respectively. Total plot-level NEP is then calculated as

$$NEP_{total} = NEP_{foliage} + NEP_{wood} + NEP_{root} + \Delta \text{ soil C}, \quad (4)$$

where Δ soil C accounts for any accumulation or depletion of carbon in the mineral soil.

2.3. Vegetation Surveys

[9] All forest vegetation was divided into three classes: trees (woody plants having a stem diameter >5 cm at a height of 1.24 m), understory (woody shrubs and saplings having a stem diameter <5 cm at a height of 1.37 m), and herbs (grasses, forbs, and bryophytes). Vegetation surveys were conducted inside four subplots regularly spaced throughout each of the 1-ha study plots. Subplot sizes ranged from 75 to 700 m^2 for trees, 5 to 75 m^2 for understory, and 2 m^2 for herbs, depending on the density and homogeneity of the vegetation. The frequency and dimensions of trees and understory in each subplot were converted to tissue mass or volume per unit area using species and site-specific allometric equations obtained from the BIOPAC database [*Means et al.*, 1994; *Van Tuyl*, 2003]. Herb mass per unit area was determined through the harvest, drying and weighing all aboveground tissue.

2.4. Wood NPP

[10] Live tree wood increment was determined for each plot using stem surveys and increment cores collected in 2001 only (as described by *Clark et al.* [2001]). For each tree in a subplot, the frequency, species, and DBH (stem diameter at 1.37 m) were recorded. For every fifth tree encountered, total height was recorded and two increment cores were taken to determine the average radial growth during the past 5 years. Plot-specific regressions relating height and radial increment to DBH allowed us to estimate the probable height and growth of trees from which no cores

Table 2. Structural Qualities of Each Age-Class Averaged Across Three Replicate Stands[a]

	Age	Stem Diameter, cm	Stem Density, ha^{-1}	Canopy Height, m	Ontogeny
Coast Range					
Initiation	12–14	11	1830	11	crowns closed, suppression not occurring, large shrub component
Young	22–40	20	1440	20	suppression and self-thinning occurring, understory absent
Mature	45–52	38	600	38	self-thinning nearly complete, understory reestablishing
Old	170–190	51	340	51	multistory canopy, gap formation, well-developed understory
West Cascades					
Initiation	13–20	10	1120	10	crowns closing, large shrub component
Young	40–70	22	740	22	self-thinning occurring, shade-tolerant understory developing.
Mature	140–170	38	340	38	self-thinning complete, well-developed. understory
Old	400–450	32	510	32	multistory canopy, gap formation, well-developed understory
East Cascades					
Initiation	9–20	10	320	10	tree crowns widely spaced, understory establishing
Young	56–89	27	300	27	crowns expanded (not closed), well-developed understory
Mature	93–106	21	980	21	some thinning occurring, some new cohort establishment
Old	190–316	30	470	30	open multistory canopy, understory often burned.

[a]Stand age defined as the ninetieth percentile of the tree stem age distribution. Stem diameter is average DBH of stems >5.0 cm DBH. Stem density is number of stems >5.0 cm DBH per ha. Height is average maximum. Sample size is three replicate plots per age class.

Table 3. Measurement Errors Associated With Each Component of NEP[a]

Component of NEP	Source of Largest Measurement Error	Average Standard Error, gC m^{-2} yr^{-1}	Average Coefficient of Variation, %	Average Resulting Error in NEP, %
Tree wood production	prediction of radial growth based on stem diameter for the portion of trees from which no increment cores were taken	58	20	20
Tree foliage production	spatial sampling error associated with optical estimates of leaf area within each plot	36	26	16
Understory wood production	predicting mass from stem diameter using non-site-specific allometry	20	317	7
Understory foliage production	uncertainty in estimates of leaf retention	8	35	2
Woody debris decomposition	spatial sampling error in field estimates of debris volume	17	25	5
Litterfall	spatial sampling error in field estimates of litterfall mass	45	33	18
Δ coarse roots	prediction of radial growth based on stem diameter for the portion of trees from which no increment cores were taken	33	57	13
Δ fine roots	standard error of a linear slope (not different from zero) fit to the change in fine root mass across the chronosequence	<1	NA	<1
Δ soil carbon	standard error of a linear slope (not different from zero) fit to the change in soil carbon across the chronosequence	5	NA	1

[a]Average SE and CV computed across all 36 plots. In the case of Δ fine root and Δ soil C, mean values were zero, and therefore a CV is not computable.

were taken. DBH and height were combined with site and species-specific allometric equations to determine the past and present volume of stemwood, branches, and bark for each tree. Tree wood volume was converted to mass using site and species-specific wood densities determined from the increment core samples. Strictly speaking, live tree wood increment as determined in this manner underestimates tree wood NPP by the live growth that any dead trees experienced in the measurement interval before dying [see *Bond-Lamberty et al.*, 2004]. However, since estimates of tree wood mortality in the Pacific Northwest are around 2% [*Harcombe*, 1986; *Grier and Logan*, 1977], we assume our estimate of live tree wood increment to equate to tree wood NPP. Understory wood production was not directly measured; rather, we assumed it to approximate 0.06 of the estimated understory wood mass [*Grier and Logan*, 1977].

2.5. Foliage NPP

[11] Overstory foliage NPP was calculated as the product of total overstory leaf mass and the canopy-average leaf retention time. Total overstory leaf mass was calculated as the product of leaf area index (LAI, expressed as hemispherical leaf area per unit ground area) and canopy-wide estimate of leaf mass per unit area. LAI for each plot was determined optically using a LAI2000 plant canopy analyzer (LICOR, Lincoln, Nebraska) as the average of 30 sample points per plot. Corrections for crown clumping were obtained using a TRAC crown gap analyzer (3rd Wave Engineering, Canada), while corrections for shoot clumping and wood interception were made as by *Law et al.* [2001a]. Canopy-wide leaf retention time and leaf mass per unit area (LMA) were determined by weighting plot and species-specific values by the frequency of overstory species in each plot, which were determined from 7–20 representative shoot samples collected in each plot. Understory foliage NPP was calculated as the understory foliage mass divided by leaf retention time, which varied from 1 year for deciduous species to 6 years for certain evergreen shrubs. Herbaceous production was assumed to be all foliage and equal to the aboveground biomass. All foliage tissue mass was converted to carbon mass by multiplying by 0.45.

2.6. Respiration From Woody Debris

[12] The volume, species, and decay class (one of five) of woody debris in each study plot was estimated using line intercept transects (four 100-m transects for woody debris >10 cm diameter and four 25-m transects for woody debris <10 and >2 cm diameter). For each piece of debris encountered in the surveys, diameter was converted to volume per unit area (using probabilistic geometry), then to mass per unit area (using a species-specific density), then to mass loss per unit time (using site, species, or diameter-specific decay constants), and finally to carbon loss per unit time (assuming 0.50 g C/g debris). Scaling constants were provided by M. Harmon (personal communication, 2001), and the details regarding the scaling of woody debris transects are given by *Harmon and Sexton* [1996].

2.7. Δ Coarse Root

[13] The annual change in coarse root (roots >2 cm diameter) was calculated as the difference between live coarse root growth minus the decomposition of dead roots attached to stumps and snags. Live coarse root growth was estimated from tree radial increment, a single region-wide allometric equation relating coarse root volume to tree diameter and species-specific wood density values (*Santantonio and Hermann* [1985] and *Van Tuyl* [2003], respectively). The decomposition of dead coarse roots was computed as volume of coarse roots attached to stumps and snags (determined, using the same allometric equations used for live trees) multiplied by decay class-specific densities and site and species-specific decomposition constants [*Janisch and Harmon*, 2002].

2.8. Δ Fine Root and Soil Carbon

[14] Measurement inaccuracies make it very difficult to directly assess a single year's change in either fine root mass

or mineral soil carbon. Consequently, we used the variation in these carbon pools across the chronosequence to estimate how much these pools may change over the course of a single year. Using this approach, neither the change in fine root mass or mineral soil carbon was discernibly different from zero. Especially notable was fine root mass that was no higher in mature forests than in the youngest age classes. Recognizing that this conclusion is subject to type II statistical error [*Davidson et al.*, 2000], we assigned an uncertainty to these zero values based on the site-wide range of pool size (see Table 3).

2.9. Ecosystem Heterotrophic Respiration

[15] Because we are more confident in our ability to estimate the components of NEP contained in equations (1) though (4) than our ability to estimate belowground heterotrophic respiration, we made estimates of total ecosystem heterotrophic respiration (HR_{total}) by subtraction according to equation (5).

$$HR_{total} = NPP_{total} - NEP_{total}, \quad (5)$$

where NPP_{total} is the sum of NPP of foliage wood and roots. HR_{total} was then further partitioned into fluxes from mineral soil, forest floor, and woody debris based on the relative magnitude of these fluxes estimated independently on each plot. Heterotrophic respiration from the mineral soil and forest floor were approximated by multiplying estimates of annual soil respiration on each study plot [*Campbell and Law*, 2004] by forest type-specific fractions representing the portion of soil respiration attributable to live roots, mineral soil, and forest floor based on in situ root separation measurements which averaged 40, 44, and 16% for root, mineral soil, and forest floor, respectively (B. E. Law, unpublished data, 2000; methods given by *Law et al.* [2001b]).

2.10. Back-Calculated C Losses

[16] An equation describing annual NEP as a function of age must include a zero point representing carbon lost to the atmosphere during the initiation disturbance if it is to be applied to a population of stands, some of which may experience such disturbances in the NEP measurement interval. Accordingly, estimates of carbon combusted as a result of slash burning following harvest were back-calculated for the youngest stands in each forest type. Without specific knowledge of what percentage of post-harvest debris actually combusted in site preparation and believing that among-site variation in debris combustion is more a function of detritus volume than the fraction combusted, we assumed that 80% of harvest debris was combusted in each plot (M. Harmon, personal communication, 2001). Consequently, NEP at age zero (NEP_0) was computed as negative 0.80 of the preharvest carbon stocks in foliage, tree branch, and understory wood, which in turn was estimated from stump inventories and site-specific allometric relationships between basal area and biomass pools.

[17] Another NEP, reflecting the heterotrophic losses occurring immediately following disturbance but prior to the re-establishment of vegetation (NEP_1), was also back-calculated for each of the youngest stands. Maximum NEP_1 at this stage was estimated as the sum of woody debris decomposition (set equal to that of the initiation stand) and soil and litter heterotrophic respiration (set equal to the average of total soil respiration among old stands on the site). Minimum NEP_1 was estimated as the sum of respiration from woody debris decomposition (recalculated from the initiation stand as if all volume was of the freshest decay class) and soil heterotrophic respiration (equal to the total soil respiration measured on the initiation stand multiplied by the site-wide fraction attributable to heterotrophic sources). The methods and values for soil respiration and separation of heterotrophic fraction are given by *Campbell and Law* [2004] and *Law et al.* [2001b], respectively.

[18] NEP_0 was located on the chronosequence at year zero, while NEP_1 was located on the chronosequence at the end of the first year following disturbance. By not including the export and fate of carbon as forest products, we limit our definition of NEP to the on-site exchange of carbon between the forest and atmosphere apart from a regional mass balance. It is important to recognize that by adopting this flux perspective, landscape NEP may be positive despite reductions in storage due to harvest.

2.11. Uncertainty Propagation

[19] We recognize that there is a great deal of uncertainty associated with each of the above-mentioned field measurements. In reporting field estimates of NEP, we believe it is more important to define the range of possible NEP values than to report a single "best estimate." When quantifying the behavior exhibited by a certain condition class (forest type and age in this study), the most useful measure of uncertainty is the variance among condition replicates. We refer to this as experimental uncertainty and calculate it for all measured parameters, including NEP, as the standard deviation among each of the three plot replicates. It is important to realize that computing this experimental uncertainty is possible only when there is true plot replication [*Hurlbert*, 1984]. When quantifying the structure of an individual study plot, the most useful measure of uncertainty is that stemming from measurement inaccuracy. We refer to this as measurement uncertainty. The measurement uncertainty associated with each component of the NEP equation was propagated through to NEP, using a Monte Carlo stochastic uncertainty estimation (M. Harmon, http://carbon-model.forestry.oregonstate.edu). In this approach, values for each component of NEP are randomly selected from a probability distribution defined by the mean and uncertainty of that component as well as the estimated covariance among components. We simulated NEP in this manner 1000 times for each plot and reported measurement uncertainty as the range in which 90% of the outcomes occurred. The sources of error assigned to each component of NEP are shown in Table 2. While these are not the sole sources of error for each parameter, our experi-